

# Shale geochemistry: a proxy for shear strength in the Pilbara?

C Kavanagh *PSM, Australia*

N Daczko *Macquarie University, Australia*

MJ Eggers *PSM, Australia*

## Abstract

*Australian iron ore is mined across the Hamersley Province, Western Australia, from open pit mines composed of mineralised interlayered strong banded iron formations (BIFs) and weaker shales. Slope design and failures are commonly controlled by shale units with low shear strengths. However, the principal controls on shale shear strength are poorly constrained. The purpose of this study is to investigate the potential relationship between shale geochemistry and shear strength.*

*The metasomatism that enriched iron in the BIFs has variably strengthened or weakened the interbedded shales. This study finds alumina ( $Al_2O_3$ ), silica ( $SiO_2$ ) and iron oxide (III) ( $Fe_2O_3$ ) to be the dominant element oxides in the shales. Shales with an alumina content <10 wt% are likely to have high strength and those >16 wt% are likely to be classified as weak. The alumina content of the shales was found to better correlate with shear strength than the defect surface condition; the latter previously having been considered the controlling factor on strength. This research permits shale shear strength to be estimated in a field environment using a portable X-ray fluorescence analyser to determine the alumina content, assisting selection of shale samples for direct shear testing.*

**Keywords:** *shale, shear strength, geochemistry, Hamersley Province*

## 1 Introduction

This paper investigates the relationship between geochemistry and the shear strength of shale bands in the iron formations of the Hamersley Group, sourced from Hardey in the Pilbara region of Western Australia (WA). The dominant strata comprising the Hamersley Group is characterised by interlayered strong banded iron formations (BIFs) and weaker shale bands, which represent a form of anisotropy (e.g. aligned bedding fabric and bedding parting defects [Nagendran & Ismail 2021]) in the rock mass. These shale bands form an important element of engineering geology across the Pilbara iron ore deposits, forming persistent zones of low shear strength in the iron formation rock mass. Shale band direct shear strength testing is typically expected to correlate well with the surface conditions of the defect being tested. For the Hamersley Group shales, surface roughness has previously been considered as the primary control causing different strength behaviours in similar rock types, where increased roughness is typically expected to correlate with increased shear strength (Hencher 1995). However, experience shows defect shear strength variation within the Hamersley Group shales does not always relate well to surface roughness or other defect conditions, such as surface infill. This suggests that another process controls shale shear strength. Previous shear strength testing of Hamersley Group stratigraphy by geotechnical company Pells Sullivan Meynink (PSM) showcases significant strength variations in individual stratigraphic units that they theorise to be driven by variations in geochemistry and mineral assemblages.

This paper forms a pilot study investigating how defect shear strength variations in the shale bands of the Hamersley Group iron formations can stem from the diverse geochemistry and mineral assemblages forming these shales. Assessing the relationship between the geochemical composition and mineral assemblages that make up these shales will build upon the work done by Maldonado et al. (2017), with a new focus on geochemistry. Understanding this geological relationship with shear strength can help improve the reliability

of pit designs by applying this knowledge in a field environment with portable geochemical analytical instruments to help field workers better select representative samples for defect shear testing.

## 2 Geology

Australian iron ore mining is heavily concentrated in WA, with more than 90% of iron ore mined from the mineralised BIFs of the Hamersley Group iron formations (Figure 1) (Jacques et al. 2002). The Hamersley Group forms part of the Mount Bruce Supergroup, a conformable sequence of volcanic and sedimentary rocks comprising the Fortescue, Hamersley and Turee Creek Groups which deposited during the late Archean and early Proterozoic (Blake & Barley 1992; Tyler & Thorne 1990; White et al. 2014).

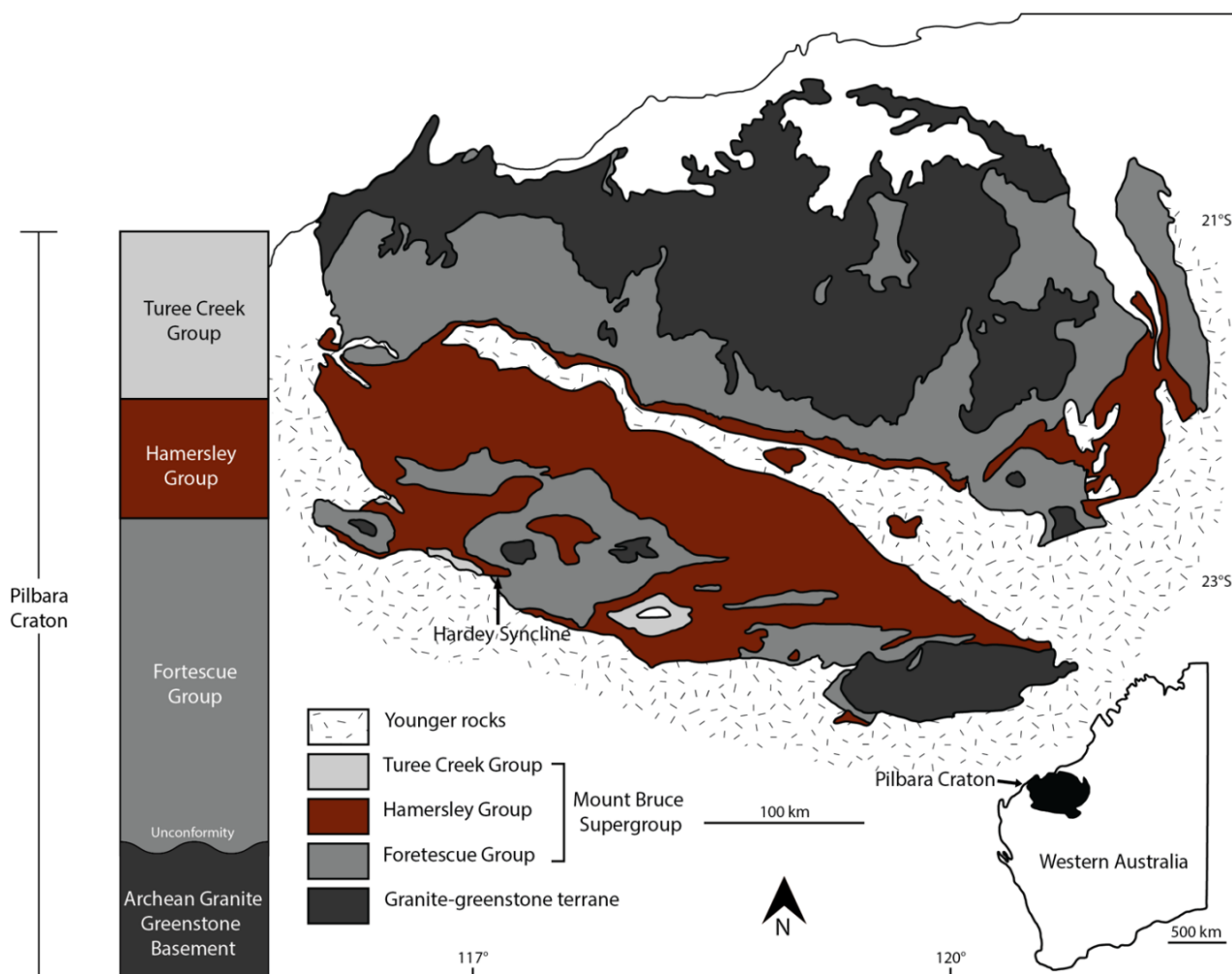


**Figure 1 Geological map and stratigraphic column of the Pilbara Craton with the Archean granite-greenstone terrane and overlying Mount Bruce Supergroup (adapted from Shibuya et al. 2010; Trendall 1990). Samples were collected from the Hardey Syncline**

The Hamersley Group conformably overlies the Fortescue Group with a thickness of up to 2.5 km, with eight formation subdivisions and numerous member subdivisions (Martin 2020; Myers 1993). The numerous stratigraphic subdivisions throughout the Hamersley Group are generally well-defined and correlated throughout the Hamersley Province. However, these rocks have experienced varying alteration styles, spatially differentiating their geochemistry and mineral assemblages across the region (Martin 2020). The rocks in the Hamersley Group are composed of extensive chemical sedimentary rocks, including iron formations with deposits of fine-grained siliciclastic and volcanic rocks such as shale, chert, dolomite and tuff (Myers 1993; Tyler & Thorne 1990). Shales for this study were taken from the eastern closure of the Hardey Syncline, an east–west trending syncline cut by numerous discrete northwest-trending faults that expose

most of the formations from the Mount Bruce Supergroup and the underlying Archean granite-greenstone rocks (Martin 2020; Occhipinti et al. 2003).

### 3 Methods

This study sampled mineralised shales within the two major iron formations (the Brockman Iron Formation and the Marra Mamba Iron Formation) and the relatively unmineralised Mount McRae Shale bound by these economic deposits (Figure 2). Thirty-nine shale samples were collected from the Hardey region in the southeast Hamersley Province of WA as a part of a commercial site investigation drilling program conducted and supervised by PSM in 2021. Valid direct shear testing results were obtained for eight samples, with testing outsourced to Trilab in Brisbane.

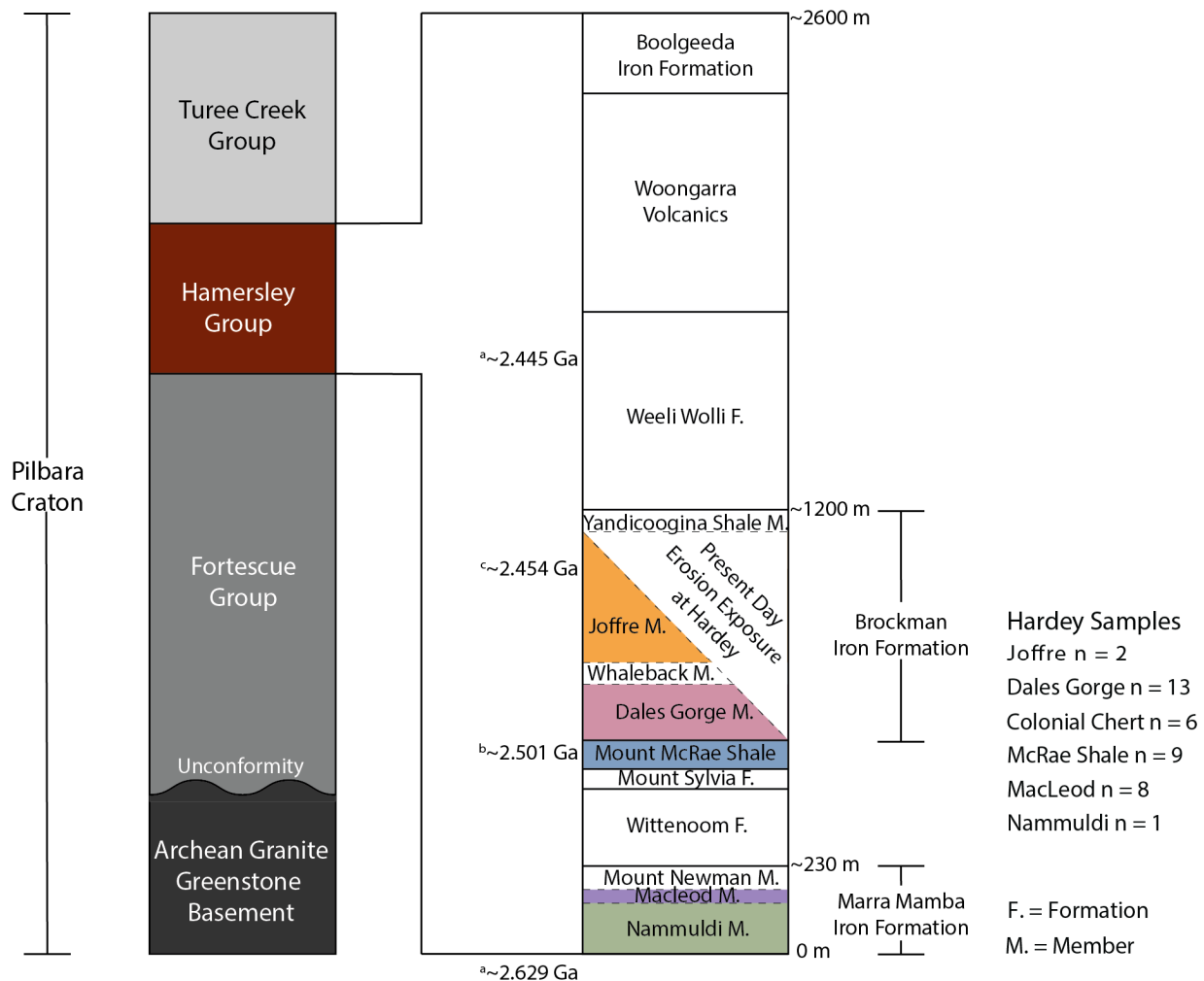


**Figure 2** Stratigraphic column of the Hamersley Group and simplified Pilbara Craton. Coloured stratigraphic units represent samples for this study, with sample counts listed under the Hardey samples ( $n$  = number of samples). Note: Colonial Chert is the youngest component of the Mount McRae Shale Member. Stratigraphic scale based on Maldonado et al. (2020). Stratigraphic ages: a = Trendall et al. (2004); b = Anbar et al. (2007); c = Pickard (2002)

All 39 samples were milled to a fine powder to undergo geochemical analysis, with stationary and portable X-ray fluorescence (pXRF) techniques used to evaluate elemental compositions. Stationary X-ray fluorescence (XRF) analysis was outsourced to the University of New South Wales, where major elements were analysed by a PANalytical Axios Advanced WDXRF 4 kW spectrometer with an end window Rh tube. pXRF analysis was conducted at Macquarie University with an Olympus Vanta handheld M Series XRF analyser using a Three Beam GeoChem method featuring three 50 kV X-ray beams, each running for 30 seconds. The pXRF analysis was also used directly on 12 intact core samples.

Legacy shale geochemistry data from regional Hamersley Group shales was compiled to compare with the local dataset produced in this study. Additionally, literature reported average geochemical compositions of Archean and Proterozoic shales were also examined. Geochemical values were collated from the North American Shale Composite, the post-Archean Australian Shale, the average Indian Archean Shale, the average Indian post-Archean Shale, and the Average Canadian Archean, Aphebian and Phanerozoic shales (Cameron & Garrels 1980; Ray & Paul 2021).

## 4 Results

### 4.1 Shale shear strengths

Legacy shale shear testing data collected by PSM for geotechnical work in the Pilbara has been compiled to show the range in shear strengths for the stratigraphic members examined in this study (Figure 3). Stratigraphic members presented include the Joffre, Dales Gorge, Colonial Chert (also known as the Footwall Zone), Mount McRae Shale and MacLeod Members.

Shear-normal stress plots show the results of the direct shear testing for this study in Figure 4. Defect conditions and assessed friction angles are reported in Table 1, with zero adopted as the cohesion value for all samples. The influence of roughness has also been examined for these samples, with the results presented in Figure 4b. The smaller sample number shows some degree of correlation with roughness, with the more extreme roughness values matching higher friction angles. However, there is variability in the shear strength which roughness does not explain.

Figure 4c presents a relationship between shear strength and the shales' alumina ( $\text{Al}_2\text{O}_3$ ) weight percent (wt%) content. The green data points represent low alumina values (<12 wt%) and define a line of best fit with a gradient that indicates friction angles higher than  $25^\circ$ , while the red points depict higher alumina content and define a line of best fit with a gradient that indicates friction angles lower than  $25^\circ$ .

**Table 1 Shale defect conditions based on field worker observations. Intact strength values: R0 = extremely weak, R1 = very weak, R2 = weak. Surface roughness values Ro1 = slickensides, Ro2 = smooth, Ro3 = defined ridges. Type values: BG = bedding, BS = bedding shear. Shape values: PL = planar, UN = undulating, CU = curved. Infill CN = clean**

Sample	Depth (m)	Weathering	Intact strength	Type	Shape	Infill	Surface roughness	Friction angle ( $^\circ$ )	Stratigraphy
SH1	14.9	Highly	R0	BG	PL	CN	Ro3	25	Joffre
SH2	64.58	Highly	R2	BG	UN	CN	Ro1	16	Joffre
SH3	62.68	Highly	R1	BS	UN	CN	Ro1	22	Dales Gorge
SH4	62.46	Highly	R1	BS	UN	CN	Ro1	24	Dales Gorge
SH5	108.97	Moderately	R1	BG	UN	CN	Ro2	21	McRae
SH7	63.1	Highly	R0	BG	UN	CN	Ro1	19	McRae
SH8	65.86	Moderately	R1	BG	UN	CN	Ro3	33	McRae
SH10	36.77	Highly	R1	BS	CU	CN	Ro2	26	MacLeod

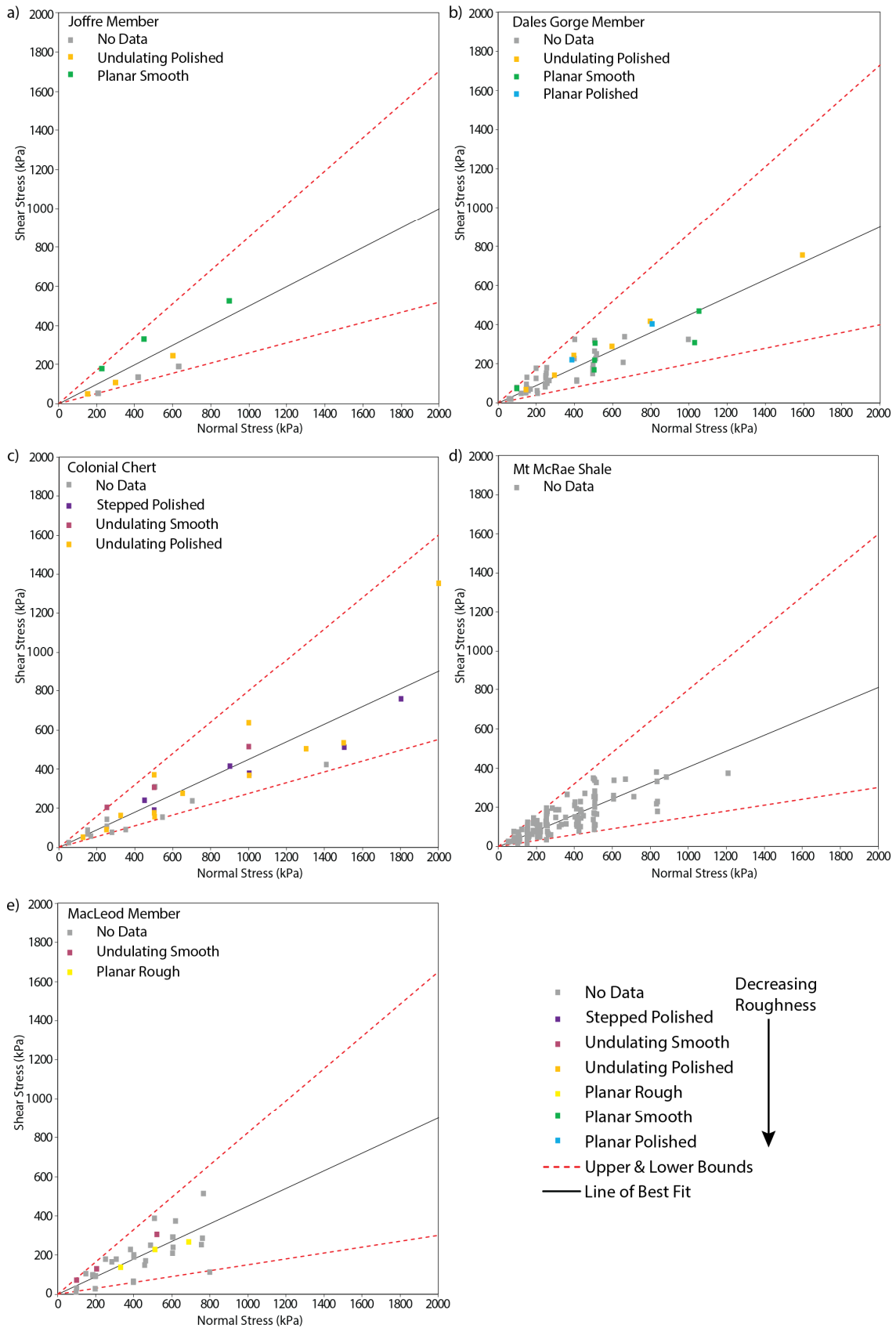


**Figure 3 Collated PSM legacy direct shear tests for the Hamersley Group Shales showing peak strength data for shale bedding defects, divided by stratigraphy. Data has been coloured by surface roughness. (a) Joffre Member Shales; (b) Dales Gorge Member Shales; (c) Colonial Chert Member Shales; (d) Mount McRae Shales; (e) MacLeod Member**

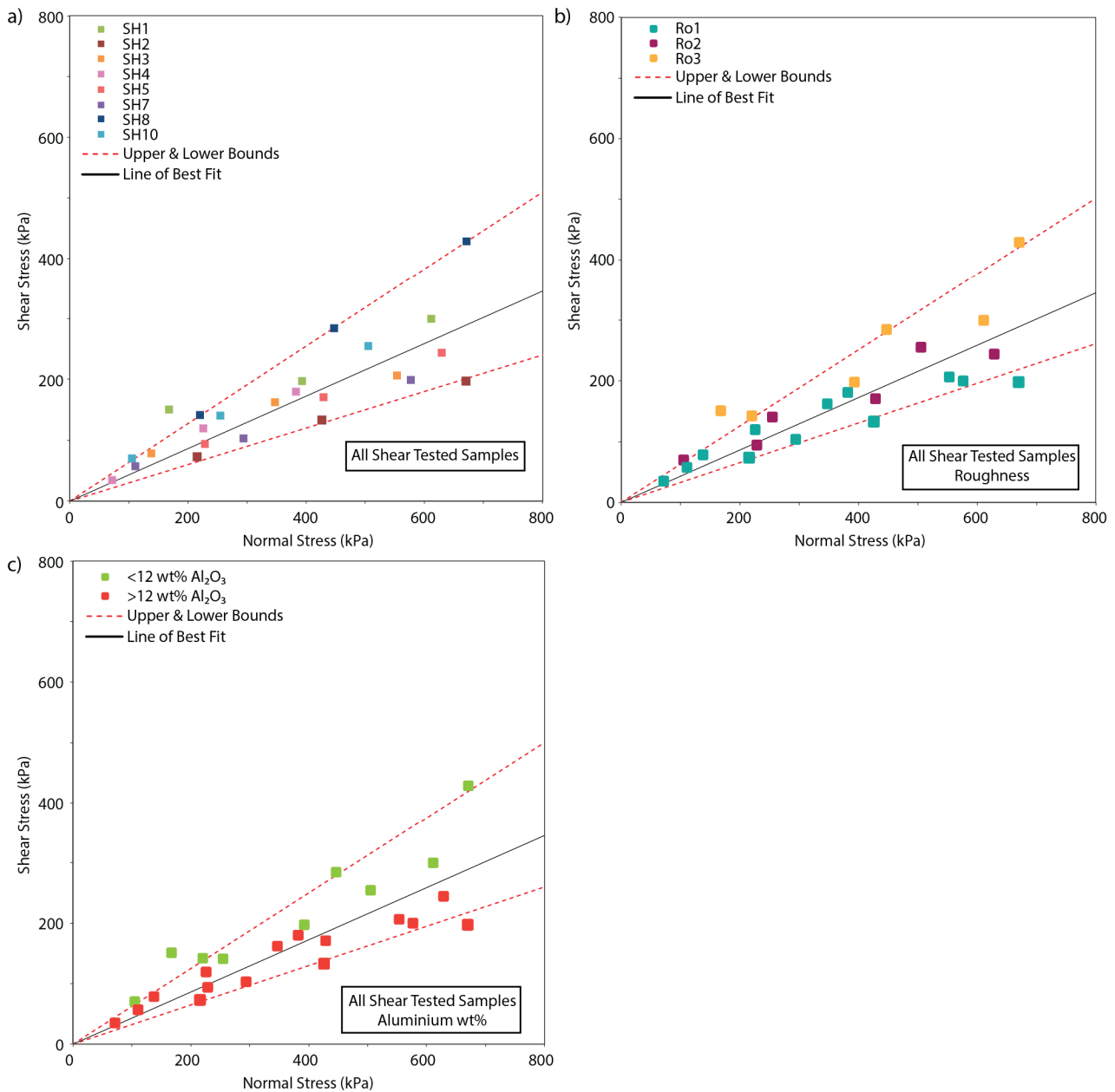


**Figure 4** Combined direct shear test results for all Hardey shale samples in this study, presented with the apparent cohesion removed. (a) All Hardey samples coloured by sample number; (b) All Hardey samples coloured by roughness; (c) All Hardey samples coloured by alumina wt% content

## 4.2 Shale geochemistry

### 4.2.1 Legacy Hamersley Group shale geochemistry and the 'average' global shale

Many of the shales of the Hamersley Group are primarily composed of three dominant element oxides: SiO<sub>2</sub>, Al<sub>2</sub>O<sub>3</sub> and Fe<sub>2</sub>O<sub>3</sub>. Other element oxides, including MgO, K<sub>2</sub>O and CaO, sometimes make up a small but significant wt% of the shales. The relationship between the three dominant element oxides for the legacy geochemical data is presented in the ternary diagram in Figure 5, coloured by stratigraphic units. Also plotted on this same diagram is the composition of various average Archean and Proterozoic shales. These representative shale values have been averaged together to create a singular starting point for an average shale, represented by the blue star (Figure 5).

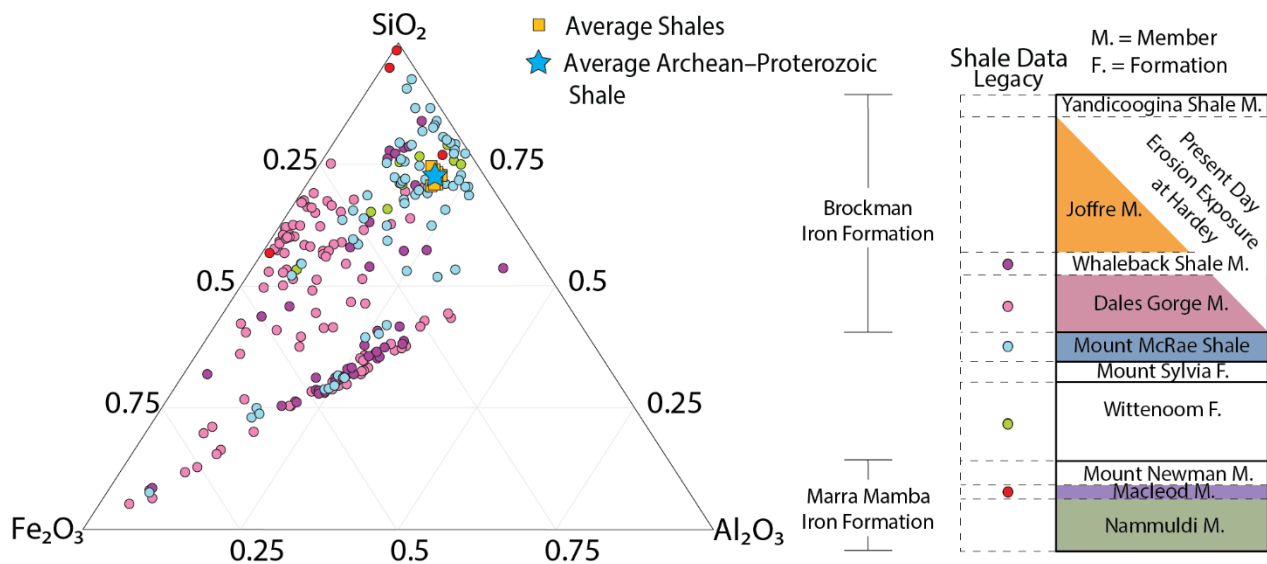


**Figure 5 Ternary plot showing SiO<sub>2</sub>, Al<sub>2</sub>O<sub>3</sub> and Fe<sub>2</sub>O<sub>3</sub> (normalised to 100 (N)), taken from legacy studies, showing mixed Hamersley Group shale band members and highlighting their compositional variations. Average shale geochemical compositions are also shown, with their combined averaged value labelled as the average Archean-Proterozoic shale (Alibert & McCulloch 1992; Cameron & Garrels 1980; Ewers & Morris 1981; Haruna et al. 2003; Kurzweil et al. 2015; Ray & Paul 2021; Simonson et al. 2009; Taylor et al. 2001; Trendall & Blockley 1970; Webb et al. 2003, 2004, 2006)**

#### 4.2.2 Hardey shales major and trace element geochemistry

The laboratory XRF major element analysis results are presented as bivariate plots in Figure 6 for all Hardey samples. These plots show Al<sub>2</sub>O<sub>3</sub> (Figure 6a) and Fe<sub>2</sub>O<sub>3</sub> (Figure 6b) plotted against SiO<sub>2</sub>, with results coloured by stratigraphic units to show the geochemical distribution within each unit. Prominent geochemical trends in these plots include silica increasing as iron oxide (III) decreases and silica increasing with increasing alumina to a 40 wt% threshold beyond which alumina decreases as silica increases. The Al<sub>2</sub>O<sub>3</sub>, SiO<sub>2</sub> and Fe<sub>2</sub>O<sub>3</sub> content of the Hardey shales show the greatest range and standard deviations of all element oxides. K<sub>2</sub>O also shows a small but significant range, but is only present in six Mount McRae Shale samples. Combined, the bulk rock SiO<sub>2</sub>, Al<sub>2</sub>O<sub>3</sub> and Fe<sub>2</sub>O<sub>3</sub> content adds up to 77.96–92.84 wt% (average 85.65 wt%). This data is normalised to 100 and plotted on a ternary diagram in Figure 6c. The missing components are mostly lost on ignition during analysis (5.07–19.44 wt%); that is, volatile substances.

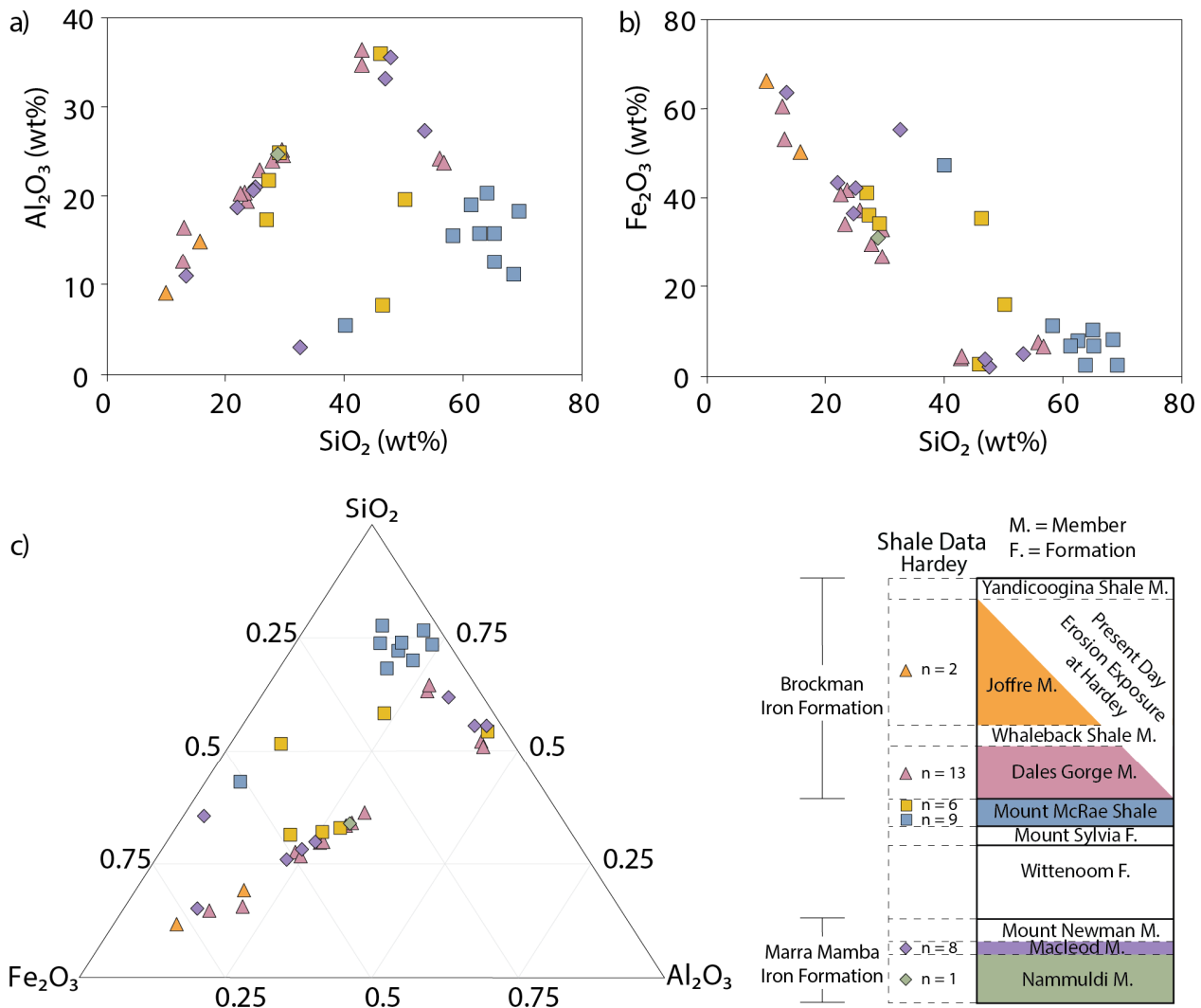


**Figure 6** (a) Bivariate plot showing the relationship between SiO<sub>2</sub> and Al<sub>2</sub>O<sub>3</sub> for the 39 samples examined here from the Hardey Syncline; (b) Bivariate plot showing the relationship between SiO<sub>2</sub> and Fe<sub>2</sub>O<sub>3</sub> for the same samples; (c) Ternary plot showing the normalised values of SiO<sub>2</sub>, Al<sub>2</sub>O<sub>3</sub> and Fe<sub>2</sub>O<sub>3</sub> for the same samples. Coloured stratigraphic units represent samples for this study, with sample counts listed under the Hardey samples (n = number of samples)

### 4.2.3 Portable X-ray fluorescence results

Results for the analysis of both powdered rock and rock core are presented in Figure 7 for the prominent and variable element oxides of SiO<sub>2</sub>, Al<sub>2</sub>O<sub>3</sub> and Fe<sub>2</sub>O<sub>3</sub>. These results are presented as a direct 1:1 comparison between the pXRF and a laboratory-run stationary XRF technique.

The powdered samples show a good correlation between the two techniques. The portable device generally overestimates both alumina and silica values, but iron oxide (III) values measured on the prepared powders (Figure 7e) are virtually the same between the two techniques. Core samples show much more variation (Figures 7b, d, f). Alumina content in the core samples is still overestimated, and shows increased variability compared to the stationary analysis. Similarly, silica content is mostly overestimated but sometimes underestimated; likely related to variation in the core area chosen for analysis. Iron oxide (III) shows some good correlation among the core samples but not at the same accuracy or precision as the powdered rock samples.



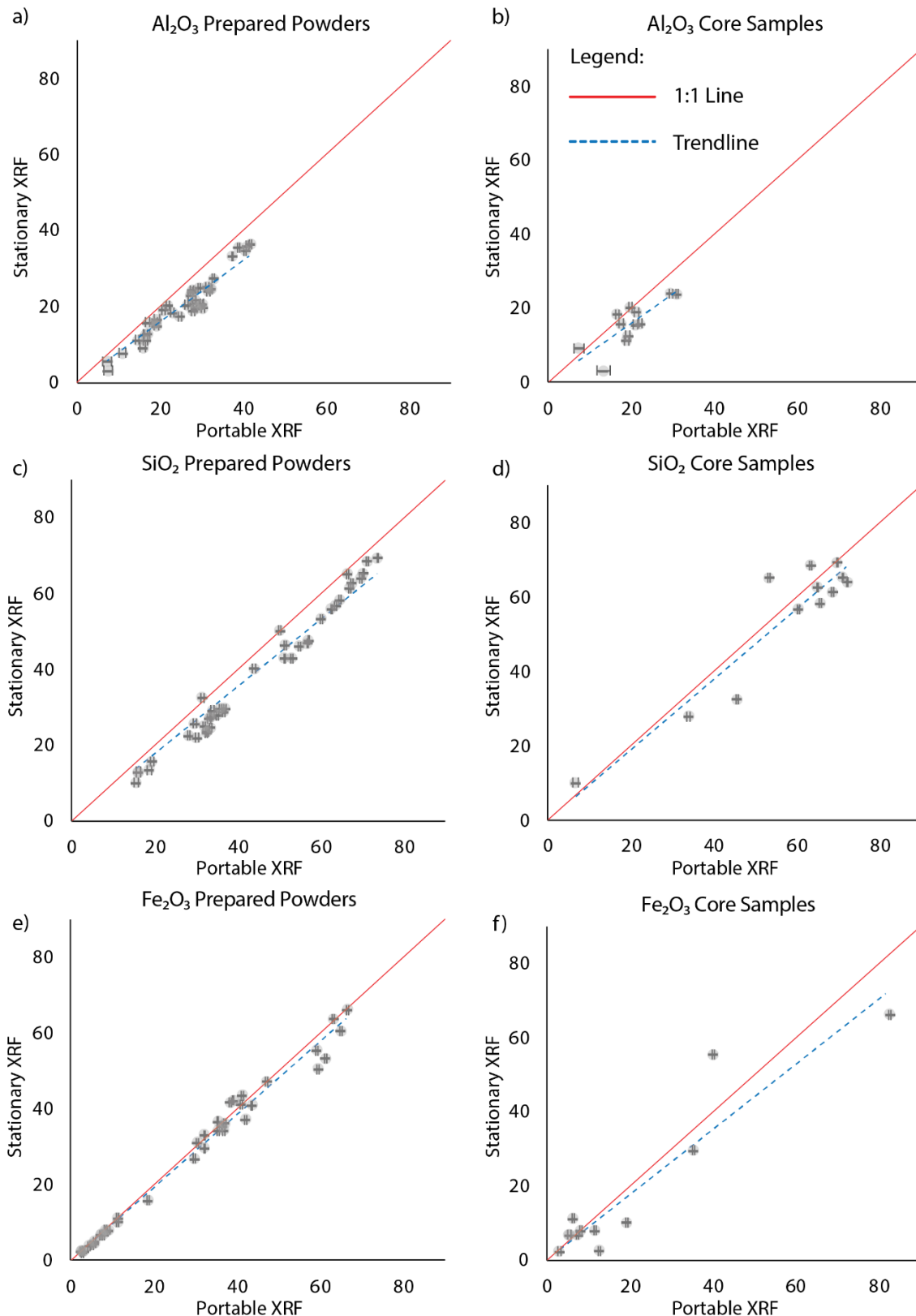


**Figure 7** Results of pXRF compared to stationary laboratory analysis. (a) Portable Al<sub>2</sub>O<sub>3</sub> results comparison for powdered and mounted samples; (b) Portable Al<sub>2</sub>O<sub>3</sub> results comparison for intact core samples; (c) Portable SiO<sub>2</sub> results comparison for powdered and mounted samples; (d) Portable SiO<sub>2</sub> results comparison for intact core samples; (e) Portable Fe<sub>2</sub>O<sub>3</sub> results comparison for powdered and mounted samples; (f) Portable Fe<sub>2</sub>O<sub>3</sub> results comparison for intact core samples

## 5 Discussion

### 5.1 Geochemical diversity of mineralised shales

Unmineralised shales of the Hamersley Province have compositions similar to the average Archean-Proterozoic shale. Mineralised shales of the Hamersley Province predominantly occur within the Brockman and Marra Mamba Iron Formations (Figure 5). These include two formal shale members of the Brockman Iron Formation (Whaleback Shale Member and Yandicoogina Shale Member) and, more commonly, shale macrobands interbedded with the BIFs, which forms all other members of the Brockman and Marra Mamba Iron Formations (Figure 5) (Trendall & Blockley 1970). The geochemistry of mineralised shale samples is diverse, ranging from near primary compositions similar to average Archean-Proterozoic shale to secondary or chemically modified compositions rich in iron oxide (III), silica and/or alumina (Figure 5). Outside of the mineralised zones, the shales are close to the average Archean-Proterozoic shale. The extensive geochemical diversity of mineralised shales of the Hardey study area reflects geochemical patterns observed in the compiled legacy geochemical data from the Hamersley Group.

Legacy geochemical testing of shale samples is skewed towards those from the two lowermost units of the Brockman Iron Formation (shale macrobands within the Dales Gorge Member and the Whaleback Shale Member) and the Mount McRae Shale, which lies immediately below the Brockman Iron Formation (Figure 5). Geochemical data is sparse for other shale samples. Generally, unmineralised shales of the Mount McRae Shale and Wittenoom Formation are stratigraphically between the two key iron formations and have similarly moderate proportions of  $\text{Al}_2\text{O}_3$  N (10–25 wt%), high  $\text{SiO}_2$  N (67–77 wt%) and low  $\text{Fe}_2\text{O}_3$  N (<15 wt%). Although their geochemistry clusters around the average shale, the regional Mount McRae Shale and Wittenoom Formation shales show minor geochemical diversity that spreads away from the average shale toward the geochemical patterns shown by mineralised shales.

Mineralised shale samples from the Hamersley Province are depleted in silica and enriched in iron oxide (III) relative to the average shale. Alumina is either depleted to low values or may be residually enriched as silica is depleted (Taylor et al. 2001). Chemically modified or metasomatised shale samples scatter around two clusters: (1) with very low  $\text{Al}_2\text{O}_3$  N (<15 wt%), high  $\text{SiO}_2$  N (55–70 wt%) and moderate  $\text{Fe}_2\text{O}_3$  N (30–40 wt%); and (2) forming a strong linear array around moderate  $\text{Al}_2\text{O}_3$  N (~25 wt%),  $\text{SiO}_2$  N (~30 wt%) and  $\text{Fe}_2\text{O}_3$  N (~45 wt%). A minor discrepancy appears between Hardey shales and more regional shales, with five samples in this study having geochemistry that is very rich in alumina and low in iron, overlapping only one sample of the Whaleback Shale Member among the legacy samples. Extreme geochemical legacy data points likely represent samples with other volumetrically significant components such as magnesium, potassium or carbon.

### 5.2 Relationship between geochemistry and shear strength

The lack of a strong relationship between the defect surface conditions and the wide range of shear strength values suggests there is likely a geochemical or mineral component generating the variation seen in shear strength. However, it is important to recognise that variability in the quality control of field logging may also have influenced this relationship with surface defect conditions.

Although this study only examined eight shear tested samples, the results indicate a potential relationship between low alumina content and stronger shear strength of shale samples. A key finding of this research is the relationship between the alumina content and shear strengths of the Hamersley Group shales. The relationship between alumina and shear strength is visualised in Figure 8, where the strongest shale samples (friction angles are equal to or greater than 25°) have  $\text{Al}_2\text{O}_3$  N contents less than 13 wt%. Conversely, the shale samples with  $\text{Al}_2\text{O}_3$  contents greater than 13 wt% are weaker, as inferred by their reduced friction angles of less than 25°.

Additional testing is required to confirm and strengthen the relationship between  $\text{Al}_2\text{O}_3$  and shear strength found by this pilot study. Given this relationship, the implementation of a process for measuring geochemistry in the field is proposed to begin building a database tailored towards individual mine sites,

allowing the relationship between the alumina and shale shear strength to be better confined. With a strengthened understanding of this relationship, geochemical testing might also aid in ensuring samples selected for laboratory testing are representative of all rock mass units or conditions encountered across a site, or they could act as a proxy for shear strength when direct shear testing data is unavailable.

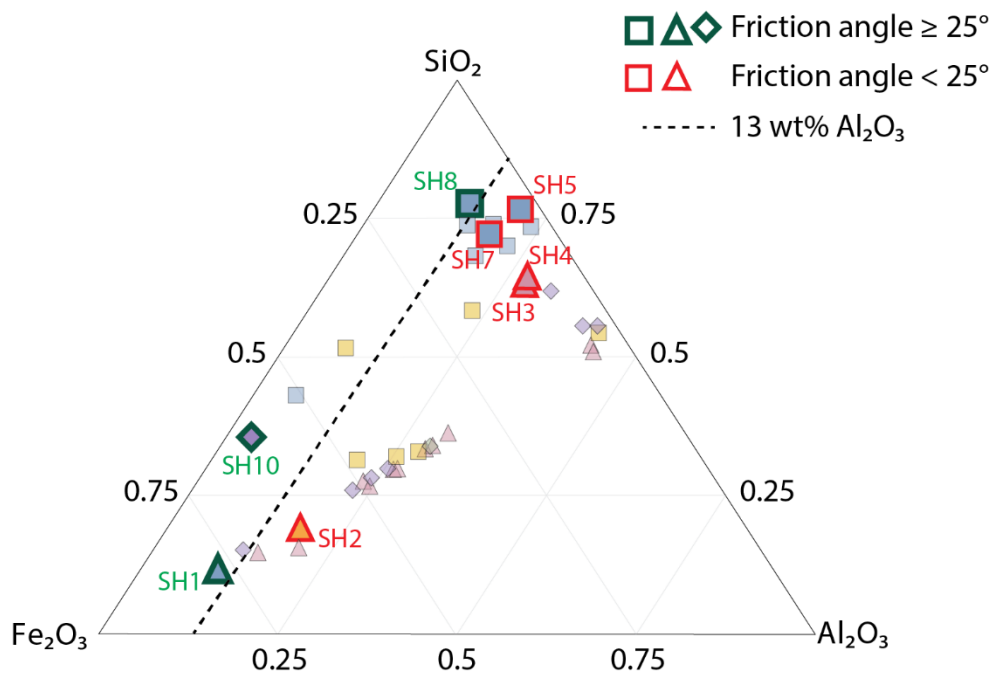


**Figure 8 Relationship between geochemistry and shear strength shown by the dashed line dividing strong shales from weak shales. Samples outlined in green have a friction angle  $\geq 25^\circ$ , while samples outlined in red have a friction angle  $< 25^\circ$ . The boundary between these samples shows a normalised alumina content of 13 wt%**

### 5.3 Geochemistry in the field

Geochemical analysis used as a proxy for shear strength has an advantage over the determination of mineral assemblages in that the bulk geochemistry of the shale samples can be relatively easily detected and quantified in a field environment. Using a laboratory geochemistry analysis to identify the best samples for shear testing would be inefficient and costly (Young et al. 2016). Instead, a more appropriate geochemical proxy method in a field environment would involve using a pXRF analyser. The pXRF has many advantages: it is easy to use, provides high-speed analysis and instant results, requires very little sample preparation and does not require regular calibration.

It is essential to recognise that the geochemical analysis performed in the field will not achieve the same level of accuracy as a laboratory analysis (Laperche & Lemièrè 2021). The pXRF has difficulty detecting light elements, particularly those with an atomic weight below 20 (Laperche & Lemièrè 2021). Elements with an atomic weight  $< 12$  cannot be detected by a pXRF, whereas aluminium, the primary element identified in this study as a proxy for shear strength, is just above this detection limit with an atomic weight of 13 (Laperche & Lemièrè 2021). Detection of aluminium (and silicon) with an atomic weight of 14 causes difficulties with detection and requires high-performance pXRF devices and a suitable configuration to ensure the best detection (Laperche & Lemièrè 2021). These difficulties in detecting lighter elements are seen in Hardey shale samples (Figure 7), with a minor overestimation of the aluminium and silicon content, while the heavier iron content was more accurately measured.

For a field study, producing homogenised powders is also inefficient. Instead, the core's most homogeneous and flat surface should be chosen to represent the sample (Young et al. 2016). Or, if the defect strength was the only component of interest, the pXRF could target only the surface of the defects rather than trying to represent the entire rock sample. Nevertheless, as long as the field operator is aware of these limitations,

the pXRF can be considered a valuable method for carrying out geochemical analysis in the field to aid in best identifying which samples should be selected for shear testing.

The use of a proxy for shear strength is a preliminary area of research where shear strength might be inferred by a shale's mineral assemblage or its geochemical composition. The decision on which samples to choose for shear testing is often conducted in the field during the process of core logging, making it imperative that the selected proxy to infer shear strength and the associated analytical technology can operate in such an environment.

This study proposes that during a pre-feasibility stage of mine pit design, a mine site engineering geologist could use a pXRF instrument to measure the iron oxide (III) and alumina content of drilled shale cores quickly and reliably. This data can be used to class samples into: (i) most likely strong (friction angle  $\geq 25^\circ$ ) where alumina content is  $< 10$  wt %; and (ii) most likely weak (friction angle  $< 25^\circ$ ) with an alumina content  $> 16\%$ . The remaining samples (10–16% alumina) can fall into either class and are the samples most in need of direct shear testing. While geochemistry can be used as a guide, it is still important to check for other influences on shear strength, such as defect surface conditions which may superimpose over the primary mineralogical control on shear strength. More accurate correlations can be developed over time for the large ore deposits, where ongoing analysis may develop into project-specific proxies to account for the variable geology across the different mine sites. These proxies may ultimately allow for the estimation of direct shear strength using the pXRF, limiting the need for extensive direct shear stress testing.

## 6 Conclusion and future work

The geochemical relationship between mineralised shales and shear strength assessed in this study shows a preliminary relationship that shales with less than 10 wt%  $\text{Al}_2\text{O}_3$  N are likely to be the strongest, and shales with greater than 16% wt%  $\text{Al}_2\text{O}_3$  N are likely to be the weakest. However, given the limitations of analytical precision, shales that straddle the boundary between 10–16 wt%  $\text{Al}_2\text{O}_3$  N are in greater need of shear testing, particularly given that they are likely to be in the shear strength range to which pit slope stability is more sensitive.

A pXRF analyser is recommended for field applied studies as it allows for a quantitative measurement of alumina to guide the selection of samples for shear testing. While the field-acquired data is not as precise or accurate as laboratory acquired data, as long as the user is aware of its limitations, the pXRF analyser is deemed to be an appropriate field technique for applying this geochemical proxy method.

While the results of this study are promising, more work is required to build upon this established relationship between shale geochemistry and shear strength. Future work should concentrate on increasing the database of both laboratory- and field-acquired geochemical data for shear tested samples to confirm the relationship and refine the preliminary geochemical cut-offs proposed here. In addition, more work needs to be done on the interrelationship between defect surface conditions, shear strength and geochemistry, where consistent and accurate datasets will have considerable impact.

## References

- Alibert, C & McCulloch, MT 1992, 'Rare earth element and neodymium isotopic compositions of the banded iron-formations and associated shales from Hamersley, Western Australia', *Geochimica et Cosmochimica Acta*, vol. 57, pp. 187–204, [https://doi.org/10.1016/0016-7037\(93\)90478-F](https://doi.org/10.1016/0016-7037(93)90478-F)
- Anbar, AD, Duan, Y, Lyons, TW, Arnold, GL, Kendall, B, Creaser, RA, ... & Buick, R 2007, 'A whiff of oxygen before the great oxidation event?', *Science*, vol. 317, pp. 1903–1906, <https://doi.org/10.1126/science.1140325>
- Blake, TS & Barley, ME 1992, 'Tectonic evolution of the late Archean to early Proterozoic Mount Bruce Megasequence Set, Western Australia', *Tectonics*, vol. 11, pp. 1415–1425, <https://doi.org/10.1029/92TC00339>
- Cameron, EM & Garrels, RM 1980, 'Geochemical compositions of some Precambrian shales from the Canadian Shield', *Chemical Geology*, vol. 28, pp. 181–197, [https://doi.org/10.1016/0009-2541\(80\)90046-7](https://doi.org/10.1016/0009-2541(80)90046-7)
- Ewers, WE & Morris, RC, 1981, 'Studies of the Dales Gorge Member of the Brockman Iron Formation, Western Australia', *Economic Geology*, vol. 76, pp. 1929–1953, <https://doi.org/10.2113/gsecongeo.76.7.1929>

- Haruna, M, Hanamuro, T, Uyeda, K, Fujimaki, H & Ohmoto, H 2003, 'Chemical, isotopic, and fluid inclusion evidence for the hydrothermal alteration of the footwall rocks of the BIF-hosted iron ore deposits in the Hamersley District, Western Australia', *Resource Geology*, vol. 53, pp. 75–88, <https://doi.org/10.1111/j.1751-3928.2003.tb00160.x>
- Hencher, SR 1995, 'Interpretation of direct shear tests on rock joints', *Rock Mechanics*, pp. 99–106.
- Jacques, AL, Jaireth, S & Walshe, JL 2002, 'Mineral systems of Australia: An overview of resources, settings and processes', *Australian Journal of Earth Sciences*, vol. 49, pp. 623–660, <https://doi.org/10.1046/j.1440-0952.2002.00946.x>
- Kurzweil, F, Wille, M, Schoenberg, R, Taubald, H & Van Kranendonk, MJ 2015, 'Continuously increasing  $\delta^{98}\text{Mo}$  values in Neoproterozoic black shales and iron formations from the Hamersley Basin', *Geochimica et Cosmochimica Acta*, vol. 164, pp. 523–542, <https://doi.org/10.1016/j.gca.2015.05.009>
- Laperche, V & Lemière, B 2021, 'Possible pitfalls in the analysis of minerals and loose materials by portable XRF, and how to overcome them', *Minerals*, vol. 11, no. 4, <https://doi.org/10.3390/min11010033>
- Maldonado, A, Dight, PM & Mercer, K 2020, 'The intact rock strength of anisotropic rocks in the Pilbara: the use of field estimations, practical limitations of calibrations and statistical bias', in PM Dight (ed.), *Slope Stability 2020: Proceedings of the 2020 International Symposium on Slope Stability in Open Pit Mining and Civil Engineering*, Australian Centre for Geomechanics, Perth, pp. 691–702, [https://doi.org/10.36487/ACG\\_repo/2025\\_44](https://doi.org/10.36487/ACG_repo/2025_44)
- Maldonado, A, Mercer, KG & Robert, A 2017, 'The relationship between mineralogy and shear strength of Pilbara Hamersley Group Shales across the weathering spectrum', *Proceedings of Iron Ore 2017*, Australasian Institute of Mining and Metallurgy, Melbourne.
- Martin, DMCB 2020, 'Geology of the Hardey Syncline—the key to understanding the northern margin of the Capricorn Orogen', *Geological Survey of Western Australia*, report 203.
- Myers, JS 1993, 'Precambrian history of the West Australian Craton and adjacent Orogens', *Annual Review of Earth and Planetary Sciences*, vol. 21, pp. 453–485, <https://doi.org/10.1146/annurev.earth.21.050193.002321>
- Nagendran, SK & Mohamad Ismail, MA 2021, 'Probabilistic and sensitivity analysis of rock slope using anisotropic material models for planar failures', *Geotechnical and Geological Engineering*, vol. 39, pp. 1979–1995, <https://doi.org/10.1007/s10706-020-01600-2>
- Occhipinti, SA, Sheppard, S, Tyler, IM, Sircombe, KN, Reddy, S, Hollingsworth, D, ... & Thorne, AM 2003, 'Proterozoic geology of the Capricorn Orogen, Western Australia — a field guide', *Geological Survey of Western Australia*, record 2003/16.
- Pickard, AL 2002, 'SHRIMP U–Pb zircon ages of tuffaceous mudrocks in the Brockman Iron Formation of the Hamersley Range, Western Australia', *Australian Journal of Earth Sciences*, vol. 49, pp. 491–507, <https://doi.org/10.1046/j.1440-0952.2002.00933.x>
- Ray, E & Paul, D 2021, 'Major and trace element characteristics of the average Indian post-Archean shale: implications for provenance, weathering, and depositional environment', *ACS Earth Space Chem*, vol. 5, pp. 1114–1129, <https://doi.org/10.1021/acsearthspacechem.1c00030>
- Shibuya, T, Aoki, K, Komiya, T & Maruyama, S 2010, 'Stratigraphy-related, low-pressure metamorphism in the Hardey Syncline, Hamersley Province, Western Australia', *Gondwana Research*, vol. 18, pp. 213–221, <https://doi.org/10.1016/j.gr.2010.01.002>
- Simonson, BM, McDonald, I, Shukolyukov, A, Koeberl, C, Reimold, WU & Lugmair, GW 2009, 'Geochemistry of 2.63–2.49 Ga impact spherule layers and implications for stratigraphic correlations and impact processes', *Precambrian Research*, vol. 175, pp. 51–76, <https://doi.org/10.1016/j.precamres.2009.08.004>
- Taylor, D, Dalstra, HJ, Harding, AE, Broadbent, GC & Barley, ME 2001, 'Genesis of high-grade hematite orebodies of the Hamersley Province, Western Australia', *Economic Geology*, vol. 96, pp. 837–873, <https://doi.org/10.2113/gsecongeo.96.4.837>
- Trendall, AF 1990, 'Hamersley Basin: geology and mineral resources of Western Australia', *Geological Survey of Western Australia*, memoir 3, pp. 163–191.
- Trendall, AF, Compston, W, Nelson, DR, De Laeter, JR & Bennett, VC 2004, 'SHRIMP zircon ages constraining the depositional chronology of the Hamersley Group, Western Australia', *Australian Journal of Earth Sciences*, vol. 51, pp. 621–644, <https://doi.org/10.1111/j.1440-0952.2004.01082.x>
- Trendall, AF & Blockley, JG 1970, 'The iron formations of the Precambrian Hamersley Group, Western Australia; with special reference to the associated crocidolite', *Geological Survey of Western Australia*, bulletin 119, pp. 1–336.
- Tyler, IM & Thorne, AM 1990, 'The northern margin of the Capricorn Orogen, Western Australia - an example of an early Proterozoic collision zone', *Journal of Structural Geology*, vol. 12, pp. 685–701, [https://doi.org/10.1016/0191-8141\(90\)90082-A](https://doi.org/10.1016/0191-8141(90)90082-A)
- Webb, AD, Dickens, GR & Oliver, NHS 2003, 'From banded iron-formation to iron ore: geochemical and mineralogical constraints from across the Hamersley Province, Western Australia', *Chemical Geology*, vol. 197, pp. 215–251, [https://doi.org/10.1016/S0009-2541\(02\)00352-2](https://doi.org/10.1016/S0009-2541(02)00352-2)
- Webb, AD, Dickens, GR & Oliver, NHS 2004, 'Carbonate alteration of the Upper Mount McRae Shale beneath the martite-microplaty hematite ore deposit at Mount Whaleback, Western Australia', *Mineralium Deposita*, vol. 39, pp. 632–645, <https://doi.org/10.1007/s00126-004-0434-z>
- Webb, AD, Dickens, GR & Oliver, NHS 2006, 'Carbonate alteration of the Upper Mount McRae Shale at Mount Whaleback, Western Australia – implications for iron ore genesis', *Applied Earth Science*, vol. 115, pp. 161–166, <https://doi.org/10.1179/174327506X139020>
- White, AJR, Legras, M, Smith, RE & Nadoll, P 2014, 'Deformation-driven, regional-scale metasomatism in the Hamersley Basin, Western Australia', *Journal of Metamorphic Geology*, vol. 32, pp. 417–433, <https://doi.org/10.1111/jmg.12078>
- Young, KE, Evans, CA, Hodges, KV, Bleacher, JE & Graff, TG 2016, 'A review of the handheld X-ray fluorescence spectrometer as a tool for field geologic investigations on Earth and in planetary surface exploration', *Applied Geochemistry*, vol. 72, pp. 77–87, <https://doi.org/10.1016/j.apgeochem.2016.07.003>

